ARTICLE

Role of Al and Mg alloying elements on corrosion behavior of zinc alloy-coated steel substrates in 0.1 M NaCl solution

Thu Thuy Pham[1,2] | Thuy Duong Nguyen[1] | Anh Son Nguyen[1] |
Thi Thao Nguyen[1,2] | Maurice Gonon[2] | Alice Belfiore[3] | Yoann Paint[3] |
Thi Xuan Hang To[1,4] (iD) | Marie-Georges Olivier[2,3] (iD)

[1]Institute for Tropical Technology, Vietnam Academy of Science and Technology, Hanoi, Vietnam

[2]Materials Science Department, Université de Mons, Mons, Belgium

[3]Materia Nova, Parc Initialis, Mons, Belgium

[4]Graduate University of Science and Technology, Vietnam Academy of Science and Technology, Hanoi, Vietnam

Correspondence
Marie-Georges Olivier, Material Science Department, Universite de Mons, Rue de l'Epargne 56, Mons 7000, Belgium.
Email: marjorie.olivier@umons.ac.be

Funding information
Académie de recherche et d'enseignement supérieur, Grant/Award Number: PRD 2020-2025: Renforcement de expertise environne; Vietnam Academy of Science and Technology, Grant/Award Number: TDVLTT.04/21-23

Abstract
The corrosion behavior and corrosion products of three zinc alloy-coated steel substrates with different Al and Mg contents such as hot-dip galvanized steel (HDG), Zn–Al-coated steel (ZA), and Zn–Al–Mg-coated steel (ZM) substrates were investigated during 168 h of immersion in 0.1 M NaCl solution. The characteristics and morphology of corrosion products on all the substrates formed during exposure to electrolyte solution were observed by X-ray diffraction, X-ray photoelectron spectroscopy, and scanning electron microscopy/energy-dispersive X-ray spectroscopy. Their electrochemical behavior was investigated by open-circuit potential, polarization curves, and electrochemical impedance spectroscopy. The addition of Al and Mg alloying elements affected the corrosion mechanism as well as the anticorrosion properties. The main crystalline corrosion products on the HDG surface were simonkolleite and zincite, while the ZnAl hydrotalcite was identified as the main corrosion product on ZA and ZM surfaces. The corrosion resistance of ZA and ZM substrates was improved compared to the HDG substrate due to the enhanced adhesion of the corrosion product layer.

KEYWORDS
corrosion products, corrosion protection, zinc alloy-coated steel

1 | INTRODUCTION

Steel and its alloys have been widely used as an industrial material; however, their corrosion in neutral and marine environments has been a major issue.[1] Zinc alloys with a more negative electrode potential than steel are used as a sacrificial anodic layer in transport sectors, buildings, and other industries.[2,3] Moreover, insoluble corrosion products of zinc alloys formed during exposure to an aggressive environment contribute to surface passivation.[3] However, the composition, solubility, compactness, and adherence of the zinc alloy corrosion products depend on the roughness and composition of the substrate surface as well as the exposure conditions.[4]

The corrosion of zinc coatings in aggressive environments containing chloride has been described by the dissolution and reprecipitation mechanisms.[2,5] Previous research studies have shown that the exposure of zinc coatings to NaCl solutions resulted in the release of Zn^{2+} cations at the anodic areas due to the dissolution of zinc surface and the formation of hydroxide anions at the cathode areas due to the reduction of oxygen and water.[2] The combinations of these Zn^{2+} cations and OH^- anions, and other ions already present in aggressive

environments, precipitated forming a complex layer of ZnO, $Zn(OH)_2$, $Zn_5(OH)_8Cl_2 \cdot 2H_2O$, and $Zn_5(OH)_6(CO_3)_2 \cdot H_2O$ on the substrate surface.[2,5] Previous studies indicated that ZnO and $Zn_5(OH)_8Cl_2 \cdot 2H_2O$ were the major corrosion products of zinc metal during exposure to NaCl solution.[5] However, Meng et al. observed a tendency of localized corrosion on the pure zinc surface during exposure to 0.9% NaCl solution.[2] Besides, Chen et al. observed the removed corrosion product layer after exposure to aggressive environments containing chloride for 21 days to study the underlying corrosion attack.[6] They revealed that zinc substrate presented cavity/hole- and groove-like morphology underneath the corrosion product layer.[6] Therefore, the pure Zn coating may not be suitable for steel protection. Designing zinc alloys containing aluminum and/or magnesium can be a promising solution to improve the local anticorrosion properties of zinc coatings.[7–12]

The corrosion behavior of Zn–Al-coated steel (ZA) and Zn–Al–Mg-coated steel (ZM) alloys and their comparison to hot-dip galvanized steel (HDG) samples in several corrosion tests in different laboratory conditions and real-life environmental conditions have been investigated.[7–12] The study of corrosion behavior of ZA (Zn and Al: 5.0 wt%), ZM (Zn, Al: 3.7 wt% and Mg: 3.0 wt%), and HDG substrates was investigated and compared during 2 years of exposure to marine, urban, and rural environments.[7] The corrosion protection of the ZM sample was improved significantly compared to those of the other two samples (the range of 2.4–3.3 times the corrosion rate).[7] Thierry et al. also reported better corrosion protection of ZM coating compared to Zn after exposure to 12 different weather locations around the world for 6 years.[9] Diler et al. studied the natural corrosion process of ZM alloy (Zn, Al: 1.5 wt% and Mg: 1.5 wt%) in the marine atmosphere and compared it to pure zinc.[8] They reported that the corrosion protection of ZM alloy was obviously better than that of pure zinc after 6 months. The corrosion performance of ZM (Zn, Al: 5.0 wt% and Mg: 1.5/4.5 wt%) and HDG coatings was checked by salt spray test with exposure to 5% NaCl.[10] The anticorrosion properties of ZM coatings were several times higher than that of HDG coating.[10] The corrosion behavior of Zn/Zn–Al double-coated steel was studied by neutral salt spray for 45 days.[11] They showed that the anticorrosion properties of Zn/Zn–Al double-coated steel substrate improved by about 4–5 times compared to pure Zn-coated steel substrate.[11] The investigation of corrosion protection of zinc alloys containing between 10% and 30% aluminum by 5% NaCl spray test also presented an improvement in their anticorrosion performance compared to pure Zn.[12] The electrochemical behavior of ZM and ZA alloy coatings by polarization curves and electrochemical impedance spectroscopy (EIS) have also been studied and compared to Zn coatings.[10–15] The electrochemical analyses indicated that the anticorrosion of Zn/Zn–Al double coating was higher than pure Zn coating during 45 days of exposure to 5% NaCl.[11] A similar result was obtained by Al-Negheimish et al. after exposure to chloride ions without/with simulated pore solution for 24 and 240 h.[12] Costa et al. investigated and compared the corrosion resistance of ZM (Zn, Al: 2.0 wt% and Mg: 1.0 wt%) coating to Zn coating by using electrochemical tests.[14] They found that the ZM coating had superior anticorrosion performance than the Zn coating.[14]

The corrosion potentials of Al and Mg were more negative than that of Zn; thus, the zinc alloys containing aluminum and/or magnesium can provide more sacrificial protection than that of pure ones. Besides, the presence of the different Al and/or Mg contents had an obvious effect on the phase structure of ZnAl (ZA) and ZnAlMg (ZM) alloys, which resulted in the intrinsic reactivity of the Zn-based coatings; thus, complex precipitated corrosion products can be formed.[15] The previous research attributed the enhanced corrosion protection of the ZA and ZM alloy coatings to the density of new corrosion products after immersion in environments containing chloride, which can impede oxygen diffusion.[3,16] They found that the formation of hydrotalcites (HTs) by coprecipitation of the corresponding ions, having the chemical formula of $[M_{1-x}^{2+}M_x^{3+}(OH)_2][A^{n-}]_{x/n} \cdot mH_2O$ (where M^{2+} and M^{3+} present divalent and trivalent metallic cations, respectively, and the A^{n-} presents interlayer anions), contributed mainly to the enhanced anticorrosion properties of the ZA and ZM alloys coatings.[3,16–18] Moreover, the enhanced performance of the ZM alloy coatings was discussed in terms of the role of unlimited Mg in the initial stages of the corrosion process.[17–19] Tsujimura et al. investigated the ZM alloy-coated steel in a cyclic corrosion test that included salt spray, drying, and humidity.[19] These authors attributed that most of the Mg on the top surface was dissolved and drained away during the corrosion process; in contrast, a significant part of dissolved Al^{3+} ions remained on the substrate surface by forming a stable mixture of corrosion products of Zn- and Al-containing Mg, which was the main reason to prevent corrosion of remaining coating and steel base.[19] Volovitch et al. suggested that the presence of dissolved Mg^{2+} ions can lead to earlier initiation of the HT formation (the ZnAl-HT solubility constant is about 5 orders of magnitude higher than that of MgAl-HT) and then the ZnAl-HT was formed by replacing Mg^{2+} ions with Zn^{2+} ions at the later stages of the corrosion process.[17] Moreover, they reported that

the lower solubility constant of the MgAl-HT was also associated with a higher number of initial nucleation regions for HT precipitation and thus the morphology of the HT crystals was more compact with better barrier properties.[17] Other research indicated that the Mg dissolution buffered the pH at cathodic regions, inhibiting the ZnO formation, limiting the efficiency of oxygen reduction, and thus the corrosion protection of these alloys was improved.[17,18]

The studies of zinc alloy-coated steel, which has been exposed to accelerated corrosion tests such as cyclic corrosion tests, salt spray, or field tests, indicated that the presence of Al and/or Mg in zinc alloy-coated steel determined their corrosive behavior and corrosion protection.[17] However, most of these studies were performed in highly corrosive conditions, and therefore, the corrosion products observed on the surface can only be representative of products (close to the end of alloys' life) for the heavily corroded coatings.[18] This can lead to erroneous conclusions about the corrosion mechanism and the influence of different alloying elements on the corrosion products.[18] Most of the publications are related to atmospheric corrosion where the conditions are controlled by droplet formation, a high concentration of dissolved oxygen, and a small content of electrolyte compared to the exposed surface. This publication aims at investigating the influence of the addition of Al and Mg to the zinc layer on the electrochemical behavior and corrosion products of the zinc alloy-coated steel after exposure to 0.1 M NaCl solution.

2 | EXPERIMENTAL METHOD

2.1 | Materials

The HDG, ZA, and ZM substrates used in this study were supplied by Arcelor Mittal (Belgium). All the substrates came from an industrial continuous line and were skin passed. The skin-passed substrates gave a specific structure to the metallic coatings. The structure depended on the skin pass roller. The chemical compositions and cross-sectional microstructure of these substrates were observed under Hitachi SU8020 finite-element scanning electron microscopy (FE-SEM). The roughness (R_a) of the top layers was studied by optical profilometry using the NanoJura instrument as described in our previous publication.[20] The chemical composition, the thickness of the top layer of these substrates, and the R_a values are given in Table 1. Before the immersion test, all the substrates were ultrasonically cleaned in acetone for 25 min, rinsed with deionized (DI) water, and further, cleaned with a $10\,g\,l^{-1}$ commercial alkaline solution (Gardoclean®) for 30 s, and finally, washed with DI water, EtOH, and dried in cooling air.

All the specimens were immersed in 0.1 M NaCl solution at room temperature for different immersion times: 24, 72, and 168 h. Finally, these panels were washed with DI water and EtOH and dried in cooling air.

2.2 | Methods and analyses

2.2.1 | Characterization

The skin-passed morphologies of all the substrates were observed using Inverted Metallurgical Microscope GX53.

The corrosion products on all the substrate surfaces after exposure to 0.1 M NaCl were analyzed by X-ray diffraction (XRD; Bruker D5000) over the 2θ range from 10° to 70° using Co Kα (wavelength = 0.1789 nm) and Fe filter.

The chemical compositions and surface morphology of all the substrates were observed using FE-SEM (Hitachi SU8020) and coupled to energy-dispersive X-ray spectroscopy (EDS; Thermo Scientific Noran System 7).

The chemical compositions of corrosion products were determined by X-ray photoelectron spectroscopy (XPS) analysis using a PHI VERSAPROBE 5000 system with a monochromatic AlKα radiation at 1486.6 eV. The XPS measurements were recorded by an X-ray source with a beam size diameter of 200 μm and power at 50 W. Atomic compositions were derived from peak areas after a Shirley baseline.

TABLE 1 Element compositions, thickness, and roughness of the top layer on the different zinc alloy-coated steel substrates.

Substrate	Element content (wt%)					Thickness (μm)	R_a (μm)
	Zn	Al	C	O	Mg		
HDG	92.1	1.2	3.9	2.8	-	11.6	0.871
ZA	82.9	9.4	3.0	4.7	-	17.5	1.225
ZM	83.6	7.2	2.4	2.8	4.0	29.0	0.012

Abbreviations: HDG, hot-dip galvanized steel; ZA, Zn–Al-coated steel; ZM, Zn–Al–Mg-coated steel.

2.2.2 | Electrochemical measurements

The electrochemical inspection concerning the corrosion behavior of all the substrates was recorded by electrochemical measurements at open-circuit potential (OCP), EIS, and potentiodynamic polarizations (Parstat Model 2273 controlled by Powersuite® software), using conventional three-electrode cell in which a platinum electrode, studied substrate with an exposed area of $1 \, cm^2$, and an Ag/AgCl (sat. KCl) were the auxiliary, working, and reference electrodes, respectively. The stability of the OCP of all samples was previously recorded for 24 h in 0.1 M NaCl. The EIS measurements were also determined in 0.1 M NaCl by using a peak-to-peak sinusoidal voltage amplitude of 5 mV in the frequency domain of 10^5 Hz to 10^{-2} Hz with 50 points. The potentiodynamic polarization curves were recorded after 24 h, 72 h, and 168 h of exposure to 0.1 M NaCl from −30 to 400 mV versus OCP (V/Ag/AgCl) at $0.2 \, mV \, s^{-1}$. Each experiment was performed at least three times to check the reproducibility.

3 | RESULTS

3.1 | Visual inspection of corroded sample surfaces

The different morphologies of skin-passed samples of the HDG, ZA, and ZM substrates can be observed in Figure 1, indicating that the structure and the roughness of the substrates were depending on the skin-pass step in the industrial process. All the studied substrates were zinc alloy-coated steel with different contents of Al and Mg (Table 1). The morphology of all original substrates showed that there were differences between the three types of zinc alloy-coated steel substrates (Figure 2). A more heterogeneous microstructure and some defects can be observed on the HDG surface (Figure 2a), which can be one of the reasons for the degradation of this substrate when exposed to a corrosion medium. A uniform morphology is observed on ZA and ZM coatings (Figure 2b,c). The Al content of the HDG, ZA, and ZM substrates was on average 1.2 wt%, 9.4 wt%, and 7.2 wt%, respectively. The presence of Mg in the ZM substrate was around 4.0 wt%. The cross-section of all the zinc alloy substrates was embedded in an epoxy resin (provided by Struers) and polished between 400 and 4000 SiC papers, and then they were analyzed by FE-SEM/EDS. The composition of zinc alloy coatings through the cross-section embedded in resin was investigated by EDS and shown in Table 2. It can be observed that the two regions had different morphology as well as Zn and Al contents on the HDG and ZA cross-sectional surfaces. In the case of the ZM substrate, three different regions can be observed on the cross-sectional surface. The Zn-rich phase regions (Region 1) with spherical flat features were surrounded by the coarse lamellar regions (Regions 2 and 3) of intermetallic phases between Mg, Al, and Zn. The thickness of the ZM layer was 29.0 μm, which was considerably higher than those of ZA (17.5 μm) and HDG
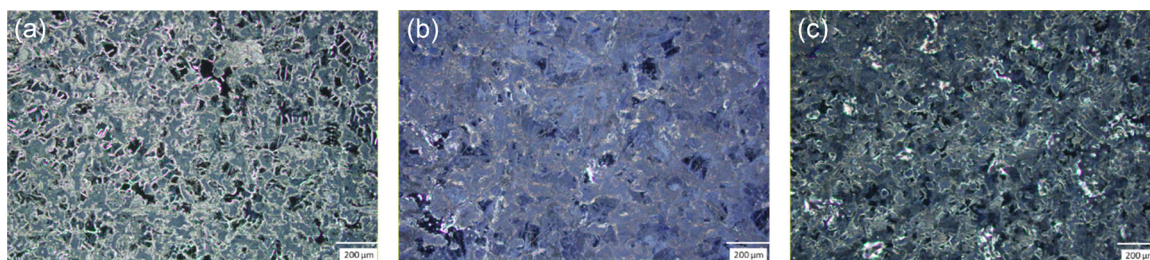

FIGURE 1 Optical photographs of skin passed hot-dip galvanized steel (a), Zn–Al-coated steel (b), and Zn–Al–Mg-coated steel (c). [Color figure can be viewed at wileyonlinelibrary.com]
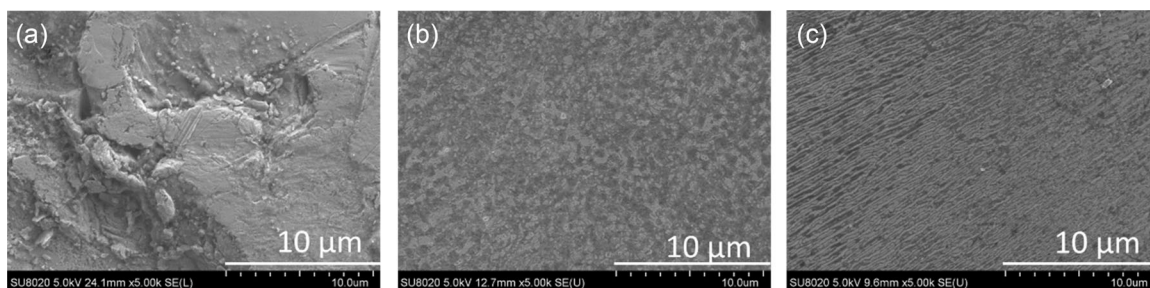

FIGURE 2 Morphology of the bare hot-dip galvanized steel (a), Zn–Al-coated steel (b), and Zn–Al–Mg-coated steel (c) substrates.

(11.6 μm) coatings (Figure 3). In contrast, the R_a value of the ZM substrate was 0.012 μm, which was significantly lower than those of other substrates (Table 1).

Figure 4 presents photographs of the surface of all the tested substrates before and after exposure to 0.1 M NaCl for 24, 72, and 168. This visual analysis of the metallic surface after different immersion times indicated the significant differences in the corrosion process of the HDG, ZA, and ZM substrates. Localized corrosion occurs and slight traces of white rust were observed on the HDG surface after 24 h. After immersion for 72 and 168 h, a gradual increase of corrosion products and two different zones on the HDG surface can be easily observed: white regions and dark gray regions. The corrosion product film in the white regions was much thicker than in the dark gray ones, confirming that corrosion products did not form a completely uniform layer in the presence of aggressive corrosive anions. In the case of the ZA and ZM substrates, the entire surface was covered with white corrosion products after immersion for 24 h, indicating localized corrosion in the initial stage. Then, it can be seen that the ZA and ZM surface substrates became more intensely colored after 72 and 168 h, confirming that the corrosion product films were getting thicker with the

immersion time increase. Moreover, it can be observed that the regions of dark gray corrosion on the ZA and ZM surface were more enlarged after immersion for a longer time.

3.2 | Characterization of corrosion products

The XRD patterns of the HDG, ZA, and ZM substrates after different immersion times are presented in Figure 5. For the HDG sample, the characteristic peaks of simonkolleite—$Zn_5(OH)_8Cl_2·H_2O/ZnCl_2·4Zn(OH)_2·H_2O$ (JCPDS No. 00-007-0155) appeared after immersion for 24 h, and the intensity of these peaks increased slightly with the increase of immersion time (Figure 5a). However, the strong peak around $2\theta = 13°$ attributed to the simonkolleite slightly shifted to a larger angle after immersion for 168 h. Moreover, recent studies presented that the theoretical locations of the 2θ value of the strongest peak of hydrozincite—$Zn_5(CO_3)_2(OH)_6$ was larger than that of simonkolleite.[8] Therefore, the hydrozincite was formed on the HDG sample surface during the later stage of the corrosion process.[8] After 24 h of immersion, the main characteristic peaks of zincite—ZnO (JCPDS No. 00-036-1451) also began to appear, but the intensity of these peaks was low, indicating that a small amount of ZnO crystallites formed on the HDG surface.[2] However, the gradual increase of these peak intensities can be easily observed with the increase in immersion time, confirming that the ZnO crystallites continued to develop and caused the layer of corrosion products to thicken, which can be observed in Figure 4. For the ZA and ZM samples, the characteristic peaks of ZnAl HT intercalated with carbonate anions—$ZnAl-CO_3$ HT (JCPDS No. 00-038-0486) were detected after 24 h immersion (Figure 5b,c).[15] Because Zn and Zn_2Mg phases preferentially dissolved for ZA and ZM alloys; therefore, the Zn^{2+} and Mg^{2+} cations were formed due to anodic reactions in process corrosion, and the local pH increased

TABLE 2 Element compositions of zinc alloy coatings.

Substrates	Element content (wt%)					
	C	O	Mg	Al	Fe	Zn
HDG-1	15.3	1.7	-	-	-	83.0
HDG-2	18.2	1.8	-	2.3	-	76.1
ZA-1	11.4	2.1	-	8.9	1.8	75.7
ZA-2	13.6	3.1	-	7.5	0.9	75.0
ZM-1	11.7	2.2	-	1.3	1.0	83.8
ZM-2	13.6	3.9	1.9	6.0	0.8	73.5
ZM-3	13.6	4.3	2.0	1.6	1.1	77.3

Abbreviations: HDG, hot-dip galvanized steel; ZA, Zn–Al-coated steel; ZM, Zn–Al–Mg-coated steel.
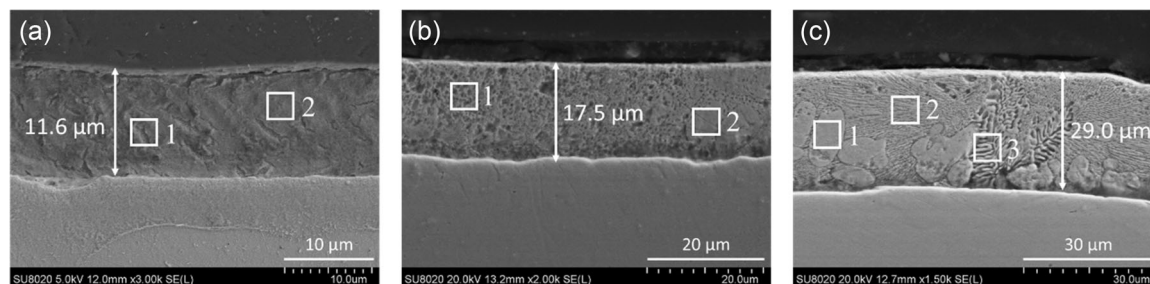

FIGURE 3 Scanning electron microscopy of the cross-sections of hot-dip galvanized steel (a), Zn–Al-coated steel (b), and Zn–Al–Mg-coated steel (c) substrates.
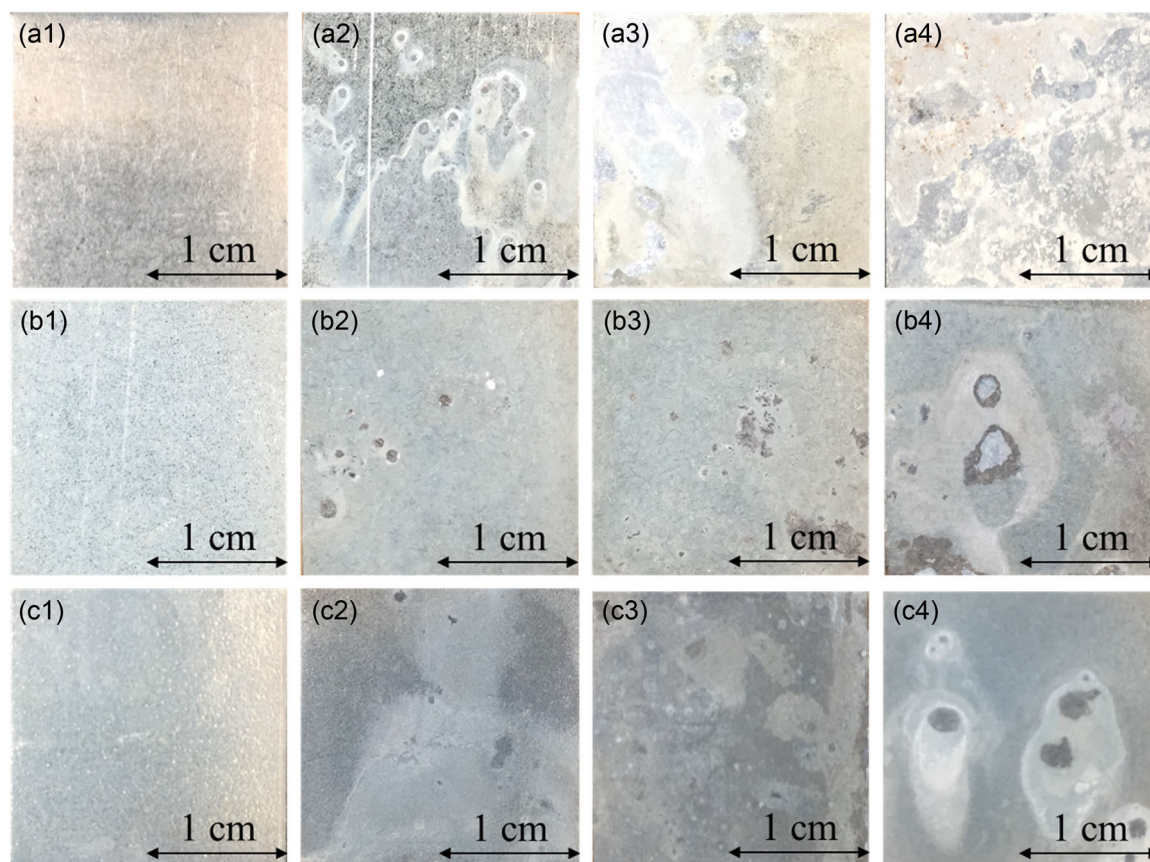
FIGURE 4 Surface of all the specimens (2×2 cm^2) exposed to 0.1 M NaCl for different immersion times: (a1–a4) hot-dip galvanized steel, (b1–b4) Zn–Al-coated steel, and (c1–c4) Zn–Al–Mg substrates for 0, 24, 72, and 168 h, respectively. [Color figure can be viewed at wileyonlinelibrary.com]

due to cathodic reaction on the Al-rich phase.[7,15] The increase of the local pH led to the formation of aluminum hydroxides on the Al-rich phase zones, and nucleation of ZnAl HT on zinc hydroxides and aluminum hydroxides. Aluminum hydroxide was considered a precursor of ZnAl-CO$_3$ HT crystal nucleation, so the existence and content of Al in zinc alloys was an influencing factor for ZnAl HT corrosion production formation.[7] The characteristic (003) and (006) peaks of ZnAl-CO$_3$ HT were not detected on the HDG surface after 24 h immersion, which may be due to the very small amount of Al in the alloy. The intensity of these ZnAl-CO$_3$ HT peaks in the ZA sample increased gradually in the remainder of the immersion process, indicating that the ZnAl-CO$_3$ HT crystallites continued to considerably grow (Figure 5b). In contrast, a slight decrease in the ZnAl-CO$_3$ HT peak intensity in the ZM sample was observed, which was caused by the partial dissolution of ZnAl-CO$_3$ HT during immersion time (Figure 5c). Besides, the characteristic peaks of ZnO were also detected in the corrosion products of the ZA sample during immersion time.[15,21] The buffering effect of Mg

dissolution from the ZM surface resulted in the inhibition of the formation of ZnO[18]; thus, their characteristic peaks cannot be observed in the XRD pattern (Figure 5c).

The composition and chemical state of corrosion products on the surface of HDG, ZA, and ZM substrates after immersion for 168 h were explored deeply by XPS analysis (Figure 6). From the XPS survey spectra of all the substrates after exposure to 0.1 M NaCl for 168 h, the typical spectral peaks, corresponding to Zn, Al, C, and O, were detected. The twin peaks of Zn 2p$_{3/2}$ (1022.5 eV) and Zn 2p$_{1/2}$ (1044.5 eV) can be observed from the XPS survey spectrum of all the samples after immersion for 168 h, which was characteristic of Zn^{2+} species.[15] Besides, the peaks of Zn LMMa (495.0 eV) and Zn LMMb Auger (474.0 eV), which confirmed corrosion products of oxidized Zn, were also observed in Figure 5.[22] The XPS spectra of C 1s (Figure 7) present the presence of the highest binding energy at about 290.5 eV, which was attributed to inorganic carbonate.[15] The other carbon-containing functional groups such as C–C and organic C–O, which were commonly attributed to surface contamination during exposure to air, were also seen
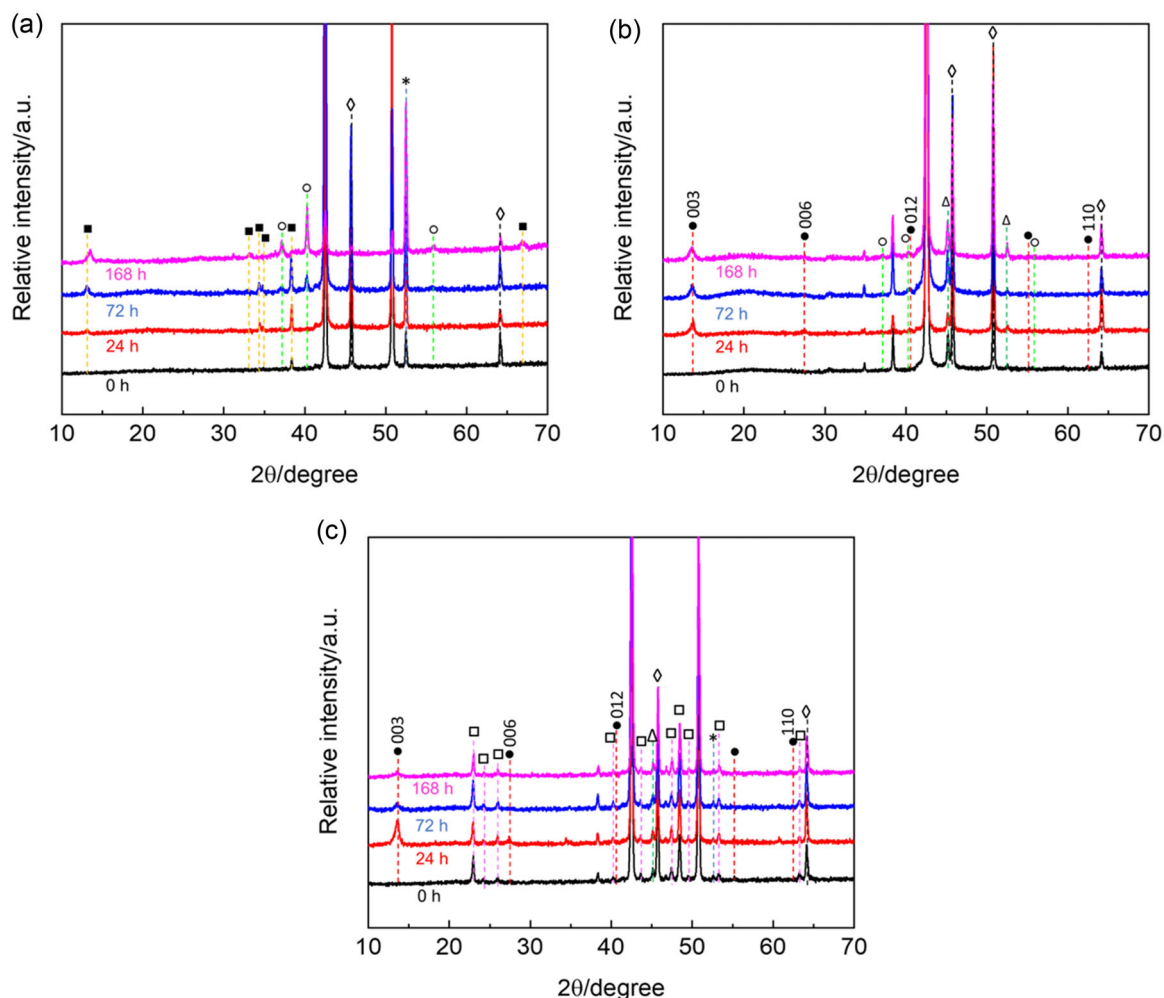
FIGURE 5 X-ray diffraction patterns of the hot-dip galvanized steel (a), Zn–Al-coated steel (b), and Zn–Al–Mg substrates (c) samples before and after exposure to 0.1 M NaCl for 24, 72, and 168 h. Peaks marked with ●, ◇, △, □, *, ○, and, ■ are contributed to ZnAl hydrotalcite, Zn, Al, MgZn$_2$, Fe, ZnO, and Zn$_5$(OH)$_8$Cl$_2$·H$_2$O/ZnCl$_2$·4Zn(OH)$_2$·H$_2$O, respectively. [Color figure can be viewed at wileyonlinelibrary.com]

from the C 1s XPS peak.[23] The peak of Cl 2p (199.0 eV) was observed from the XPS survey spectra of the HDG substrate (Figure 6a), confirming the formation of simonkolleite on the HDG surface.[2] In contrast, chloride was not detected by XPS on the ZA and ZM surfaces after immersion, which indicated that the chloride-containing corrosion products were not present on these surfaces. The peak of Al 2p (74.5 eV) was characteristic of Al^{3+} species, which was detected on the ZA and ZM surface; however, this peak was not observed on the HDG surface. Combined with the XRD result, it can be concluded that the ZnAl-CO$_3$ HT grew and covered the ZA and ZM surfaces; however, this corrosion product did not appear on the HDG surface. Moreover, the peaks of Mg 2p (50.0 eV) and Mg KLL Auger (300.0 eV), corresponding to the Mg corrosion products such as MgO, Mg(OH)$_2$, and MgCO$_3$, were detected on the ZM surface (Figure 6c).[4] The amount of corrosion products of the oxidized Mg on the ZM surface was probably very small because they cannot be detected by XRD.

The corrosion composition and morphology of all the samples were observed by SEM/EDS and EDS maps for the different immersion times (Figures 8–11 and Table 3). The corrosion morphology of all the substrates depended on the composition and morphology of the sacrificial layer; therefore, different corrosion behaviors were observed between the HDG, ZA, and ZM substrates (Figure 8). The heterogeneous simonkolleite corrosion product layer was formed on the HDG surface, while the ZA and ZM surfaces were covered by the continuous HT nanosheets after immersion for 24 h. The HT corrosion products formed on the ZM surface were more uniform and denser than on the ZA surface after 24 h explained by the presence of Mg^{2+} ions, which can lead to earlier initiation and a higher number of initial nucleation regions of the MgAl HT precipitation compared to ZnAl-HT one.[17,18] Then, due to the lower solubility constant of the MgAl HT, the ZnAl HT was grown on the ZM substrate by the exchange reaction of Zn^{2+} and
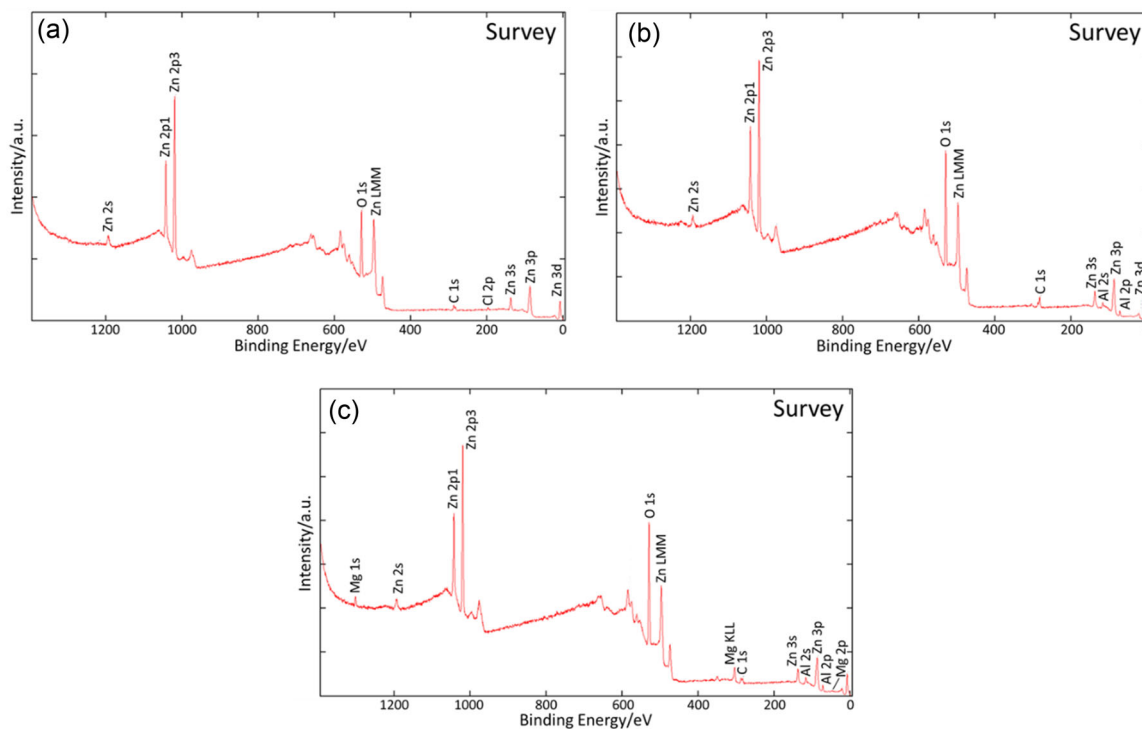
FIGURE 6 X-ray photoelectron spectroscopy survey spectra of hot-dip galvanized steel (a), Zn–Al-coated steel (b), and Zn–Al–Mg-coated steel (c) surfaces after immersion for 168 h in 0.1 M NaCl. [Color figure can be viewed at wileyonlinelibrary.com]
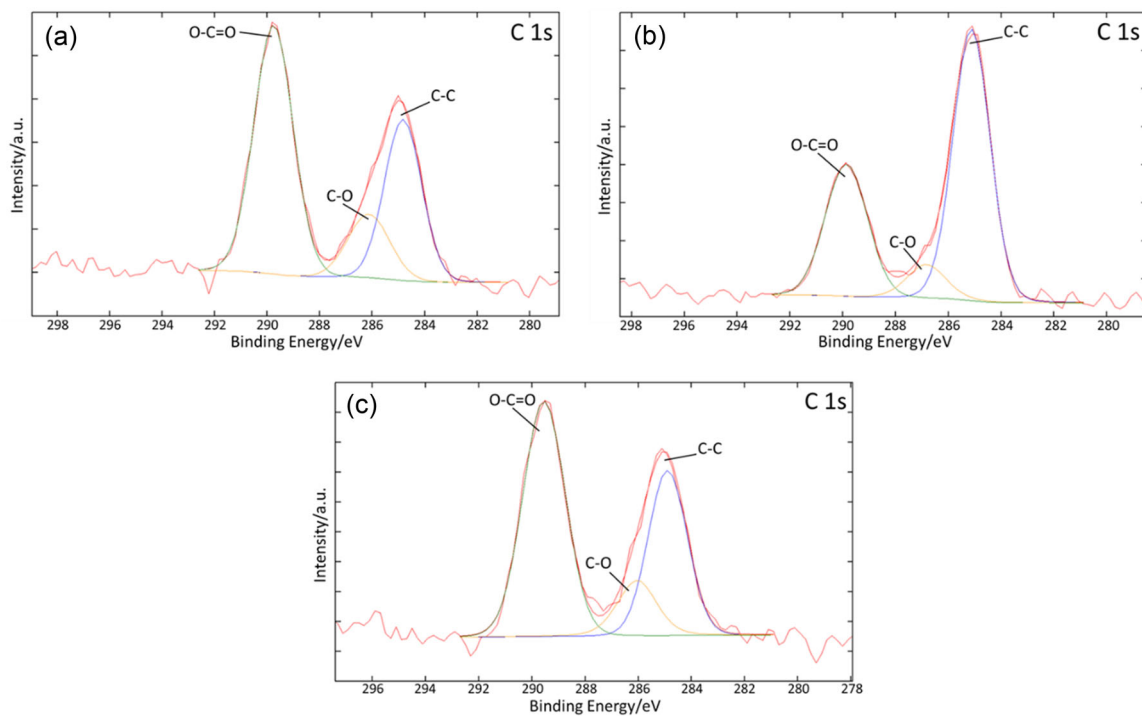

FIGURE 7 X-ray photoelectron spectroscopy spectra of C 1 s of the hot-dip galvanized steel (a), Zn–Al-coated steel (b), and Zn–Al–Mg-coated steel (c) surfaces after immersion for 168 h in 0.1 M NaCl. [Color figure can be viewed at wileyonlinelibrary.com]
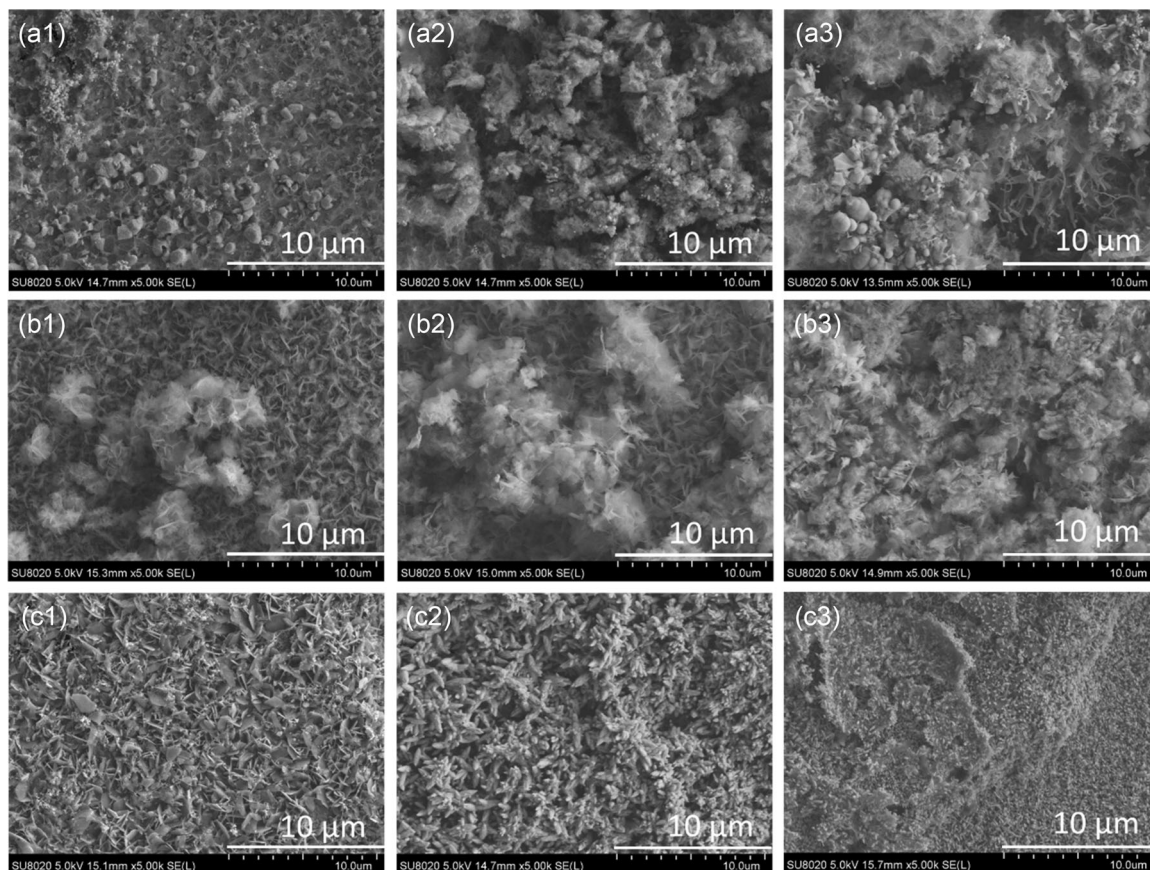
FIGURE 8 Morphology of the hot-dip galvanized steel (a1–a3), Zn–Al-coated steel (b1–b3), and Zn–Al–Mg-coated steel (c1–c3) substrates after 24, 72, and 168 h of immersion in NaCl.
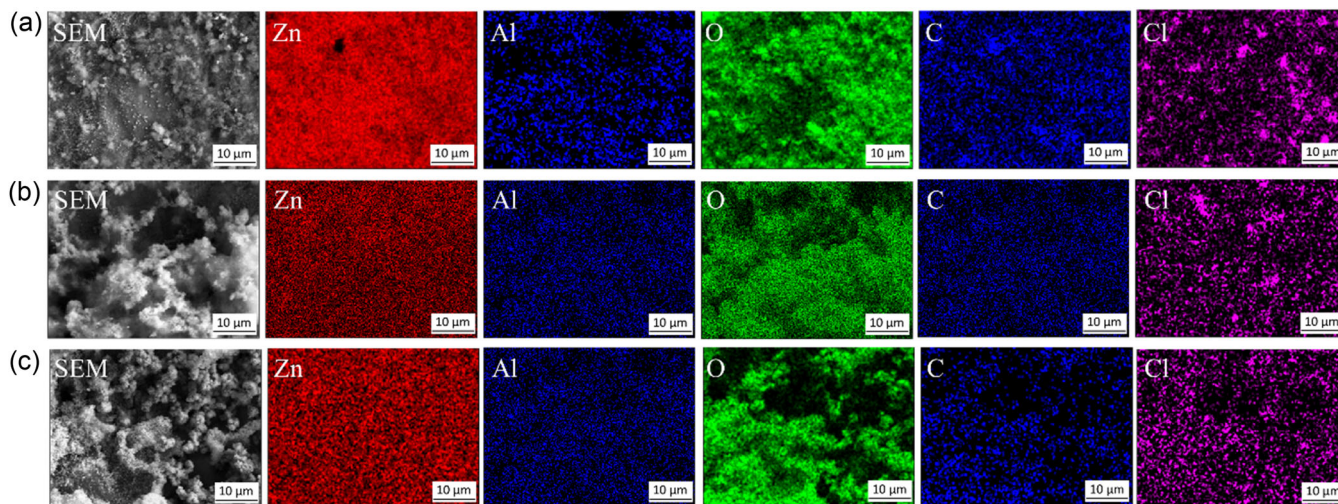
FIGURE 9 Energy-dispersive X-ray spectroscopy maps of the HDG surface (a–c) after exposure to 0.1 M NaCl for 24, 72, and 168 h, respectively. [Color figure can be viewed at wileyonlinelibrary.com]

Mg^{2+}.[17,18] Most of the MgAl HT crystals may have turned into ZnAl HT after exposure to 0.1 M NaCl for 24 h, so they cannot be observed by XRD. This effect can be probably explained by the buffering effect related to

the magnesium corrosion in the alkaline region. For longer immersion time, thicker, porous corrosion product layers were formed on the HDG and ZA surfaces (Figure 8a,b). In contrast, the corrosion product layers of
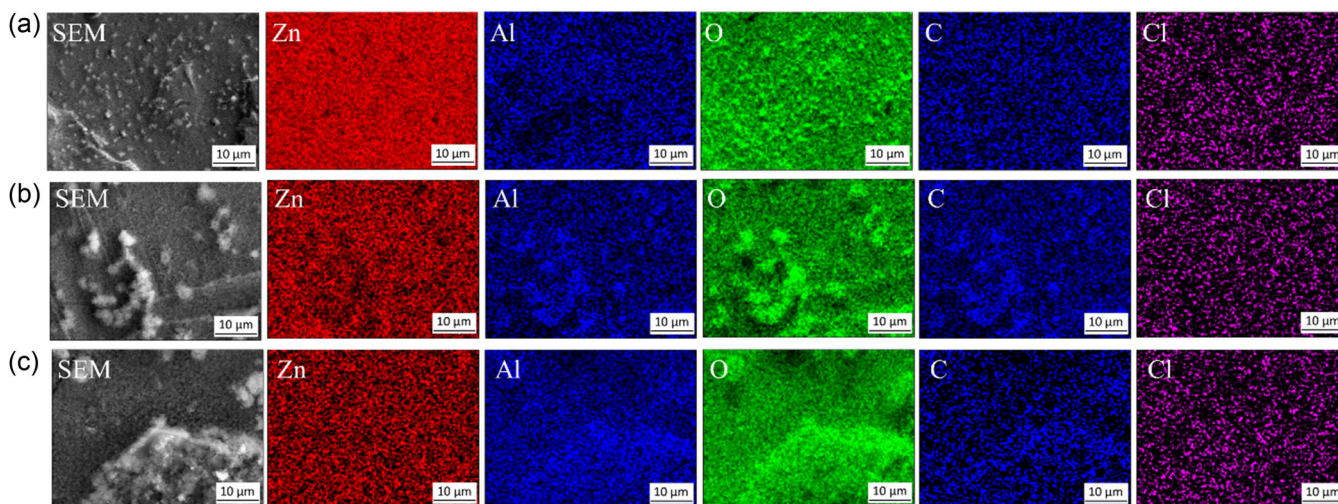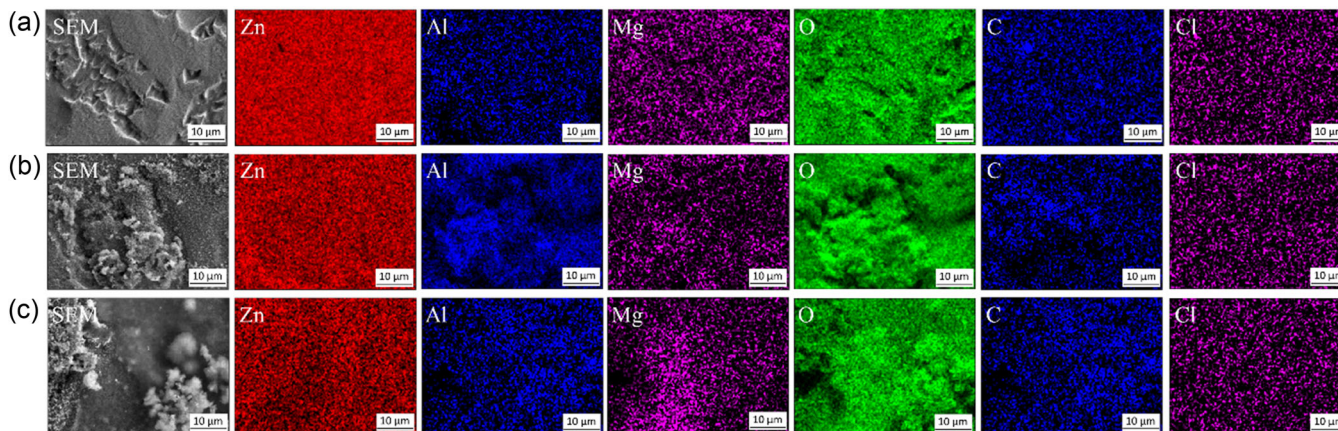
FIGURE 10 Energy-dispersive X-ray spectroscopy maps of the ZA surface (a–c) after exposure to 0.1 M NaCl for 24, 72, and 168 h, respectively. [Color figure can be viewed at wileyonlinelibrary.com]

FIGURE 11 Energy-dispersive X-ray spectroscopy maps of the ZM surface (a–c) after exposure to 0.1 M NaCl for 24, 72, and 168 h, respectively. [Color figure can be viewed at wileyonlinelibrary.com]

the ZM substrate were nonporous and more compact after the same immersion time (Figure 8c). Moreover, these HT nanoplates of corrosion products were sharper for a longer time, which may be due to their partial dissolution. The effect of Mg^{2+} ions stabilized HT crystals on the ZM surface and inhibited ZnO formation; thus, the corrosion production on the ZM surface was a more compact and denser morphology than those of the two other samples.[18] As shown in Table 3, the Zn, Al, O, C, and Cl contents of HDG, ZA, and ZM substrates altered with time. The Zn contents detected on all the substrate surfaces reduced over time. In contrast, the surfaces became richer in O content, which can be due to more oxygen-containing products on the surface of all substrates. For the HDG surface, the Cl content reduced significantly, and the C content increased slightly at prolonged immersion, indicating that the simonkolleite

was partially transformed into zinc hydroxide carbonate. The Mg content on the ZM surface reduced significantly to reach 0.3 wt%, confirming that a considerable part of the Mg^{2+} ions was dissolved and did not participate in the growth of corrosion products.[19] The Al content observed on the ZA surface increased from 4.4 to 9.0 wt%, while the Al content on the ZM surface decreased from 3.2 to 2.6 wt%. These results are consistent with the SEM results (Figure 8), the ZnAl HT formation on the ZA surface increased versus time; in contrast, the amount of ZnAl HT nanoplates on the ZM surface was dissolved. Moreover, the corrosion composition of all the samples was studied by EDS maps (Figures 9–11). The EDS maps of the HDG surface after immersion for 24 h showed that some regions enriched in Cl were observed with high intensity of Zn and O, confirming the coexistence of zincite and simonkolleite at the corroded sites (Figure 9a). The zones,

TABLE 3 Element contents of the HDG, ZA, and ZM substrates after exposure to 0.1 M NaCl for 24, 72, and 168 h.

Sample	Element content (wt%)					
	Zn	Al	O	C	Cl	Mg
HDG—24 h	70.3	0.8	25.5	1.7	1.1	-
HDG—72 h	67.8	-	27.1	1.7	0.8	-
HDG—168 h	65.8	-	31.9	1.9	0.4	-
ZA—24 h	76.1	4.4	17.7	1.8	0.2	-
ZA—72 h	50.5	8.6	38.7	2.0	0.2	-
ZA—168 h	44.5	9.0	43.0	2.1	0.1	-
ZM—24 h	74.0	3.2	18.9	2.2	0.1	1.4
ZM—72 h	71.7	2.8	22.1	2.2	0.2	0.7
ZM—168 h	70.2	2.6	24.2	2.2	0.2	0.3

Abbreviations: HDG, hot-dip galvanized steel; ZA, Zn–Al-coated steel; ZM, Zn–Al–Mg-coated steel.

which were enriched in O, were extended after 72 and 168 h, indicating that the corrosion product layer containing oxygen as ZnO, $Zn_5(OH)_8Cl_2 \cdot H_2O/ZnCl_2 \cdot 4Zn(OH)_2 \cdot H_2O$, and $Zn_5(CO_3)_2(OH)_6$ was thicker and almost covered the HDG surface. The even distribution of all the elements on the ZA and ZM surfaces after 24 h indicated the relatively homogeneous corrosion product layer. The O, C, and Al distributions were almost identical on the ZA and ZM surfaces after 72 and 168 h, confirming that ZnAl-CO$_3$ HT was the main corrosion product for these immersion times.

3.3 | Electrochemical corrosion behavior

The OCP stability of all the substrate samples was checked during exposure to 0.1 M NaCl for 24 h (Figure 12). The OCP of the ZM sample was lower than those of HDG and ZA samples during the first 6 h of the surveyed period, indicating that the ZM coating can provide more sacrificial protection than those of the other two coatings due to the addition of magnesium. The OCP of all substrates decreased slightly and varied noticeably through immersion of 6 h, which reflected a significant change on these surfaces with the corrosion process. The dissolution of these top layers of the substrates and self-acceleration of anodic dissolution was the main cause of unstable electrode potential. At the end of immersion time, the OCP values of HDG and ZA samples were stabilized at around −1.05 V versus Ag/AgCl. The OCP values of the ZM sample increased sharply and were higher than those of other samples
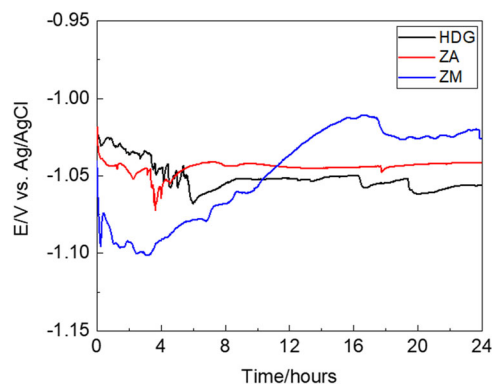

FIGURE 12 OCP of the HDG, ZA, and ZM substrates during exposure to 0.1 M NaCl for 24 h. HDG, hot-dip galvanized steel; OCP, open-circuit potential; ZA, Zn–Al-coated steel; ZM, Zn–Al–Mg-coated steel. [Color figure can be viewed at wileyonlinelibrary.com]

after 12 h of immersion, before remaining stable at around −1.02 V versus Ag/AgCl in the remainder of the given period. The OCP values of the ZM sample at the end of the surveyed period were gradually higher than those of other substrates. The previous studies showed that the HT corrosion product layer on zinc alloy substrates acted as an anodic inhibitor;[15] Moreover, the characterization results confirmed that a uniform and dense corrosion product layer was formed on the ZM surface compared to two other substrates after 24 h. They can be the main reason for the higher OCP values of ZM substrate after exposure for a longer time.

The polarization curves were used to investigate the electrochemical behavior of all substrates after exposure to 0.1 M NaCl for 24, 72, and 168 h (Figure 13). The results of corrosion potential (E_{corr}) and corrosion current densities (i_{corr}) of all samples are listed in Table 4. The E_{corr} values of all substrates moved toward more positive values with the extension of exposure to NaCl solution, suggesting that anodic inhibitor films were developed on all the surface substrates. The i_{corr} values of ZM samples were considerably lower than those of HDG and ZA samples during immersion time (Table 4), confirming that the ZM coating can provide higher corrosion resistance than those of the other two sacrificial layers. This can explain why the addition of Mg leads to more dense and compact corrosion products, hence enhanced corrosion protection.[10] The i_{corr} values of the HDG sample after 24, 72, and 168 h were 2.40, 2.01, and 3.08 $\mu A\,cm^{-2}$, respectively, indicating that the corrosion protection of this coating increased moderately after 72 h before reducing significantly after 168 h. In contrast, the i_{corr} values obtained in the case of ZA and ZM coatings decreased gradually over time, confirming that the corrosion protection of ZA and
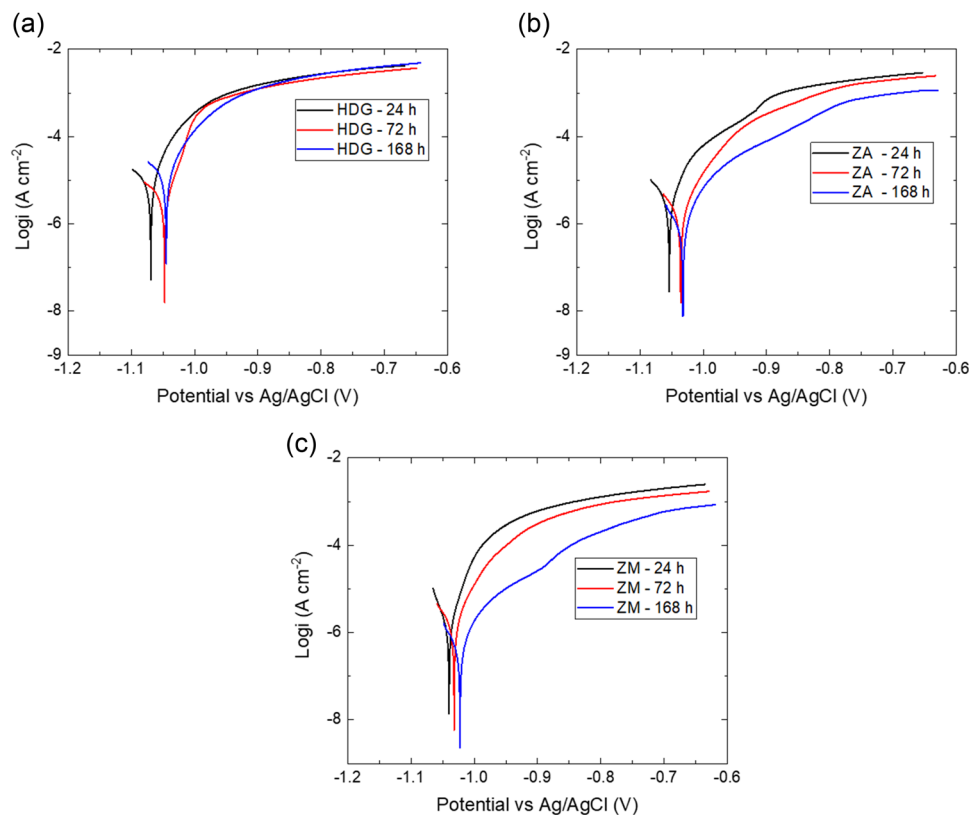
FIGURE 13 Potentiodynamic polarization curves of the HDG, ZA, and ZM substrates during exposure to 0.1 M NaCl. HDG, hot-dip galvanized steel; ZA, Zn–Al-coated steel; ZM, Zn–Al–Mg-coated steel. [Color figure can be viewed at wileyonlinelibrary.com]

TABLE 4 E_{corr} and i_{corr} derived from the polarization measurement of the HDG, ZA, and ZM substrates after exposure to 0.1 M NaCl for 24, 72, and 168 h.

Samples	E_{corr} (V/Ag/AgCl)	i_{corr} (μA cm^{-2})
HDG—24 h	−1.06 ± 0.05	2.40 ± 0.04
HDG—72 h	−1.05 ± 0.06	2.01 ± 0.02
HDG—168 h	−1.04 ± 0.04	3.08 ± 0.07
ZA—24 h	−1.05 ± 0.03	2.00 ± 0.03
ZA—72 h	−1.04 ± 0.04	1.04 ± 0.06
ZA—168 h	−1.03 ± 0.06	0.89 ± 0.02
ZM—24 h	−1.03 ± 0.03	1.81 ± 0.03
ZM—72 h	−1.03 ± 0.05	1.12 ± 0.02
ZM—68 h	−1.02 ± 0.03	0.75 ± 0.05

Abbreviations: HDG, hot-dip galvanized steel; ZA, Zn–Al-coated steel; ZM, Zn–Al–Mg-coated steel.

ZM coatings increased due to the nature of the formed corrosion products.

The corrosion resistance and corrosion protection mechanism of all the substrates were also studied by EIS measurements during exposure to 0.1 M NaCl (Figure 14 and Table 5). The impedance diagrams of HDG substrates presented two time constants after 2 h (Figure 14a,b), thus the model $R_s(CPE_f(R_f(CPE_{dl}R_{ct})))$ (Figure 15a), where R_s is the solution resistance, R_f and CPE_f are representatives of the outer film, and, R_{ct} and CPE_{dl} are related to charge transfer resistance and the double layer capacitance, was used for the EIS fitting results. However, only one time constant can be seen for the HDG substrate after 24 h, indicating that the corrosion products merged into one layer.[20] The fitted model $R_s(CPE_{dl}R_{ct})$ was selected for the HDG substrate after an exposure time of 24 h (Figure 15b). Combining with the results from XRD, XPS, and SEM/EDS analysis of the corrosion product, the mixed corrosion layer of simonkolleite and ZnO covered all the HDG surface substrate after 24 h. Moreover, the R_{ct} value of the HDG substrate after 24 h was slightly higher than that of one after 2 h (Table 5), confirming that the anticorrosion properties of this substrate were enhanced by the corrosion product layer after 24 h. Two time constants were observed for the HDG substrate after 72 and 168 h and the same EEC $R_s(CPE_f(R_f(CPE_{dl}R_{ct})))$ was used (Figure 15a). The HDG R_f values increased to 2241 Ω cm^2 after 72 h and reduced sharply to 1329 Ω cm^2 after 168 h. Moreover, the HDG R_{ct} values decreased obviously to 877 and 401 Ω cm^2 after 72 and
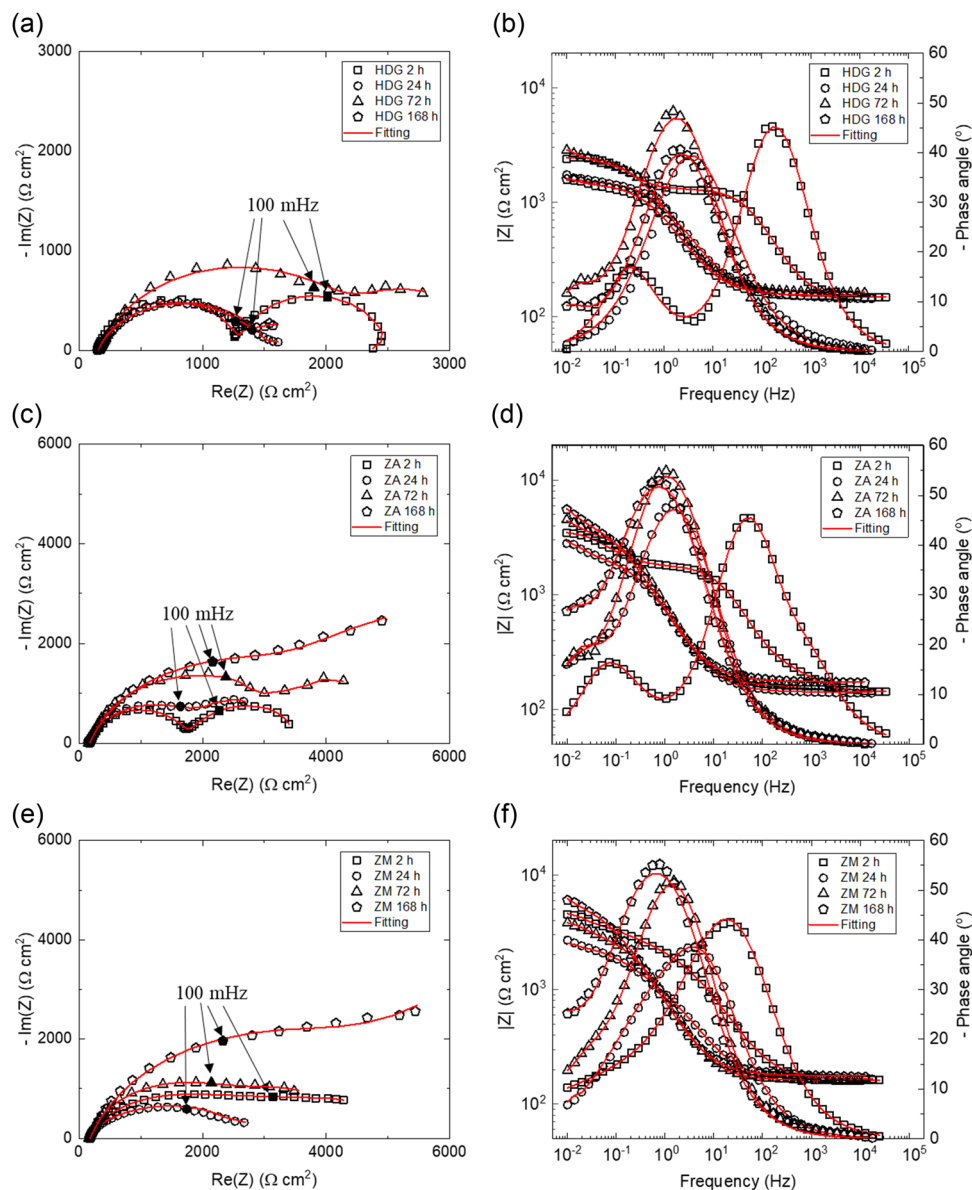
FIGURE 14 Nyquist and bode plots of the HDG, ZA, and ZM substrates during exposure to 0.1 M NaCl. HDG, hot-dip galvanized steel; ZA, Zn–Al-coated steel; ZM, Zn–Al–Mg-coated steel. [Color figure can be viewed at wileyonlinelibrary.com]

168 h, respectively. Because the corrosion products such as simonkolleite and ZnO have porous structures and poor adhesion to the surface substrate, aggressive species such as Cl^- can penetrate and destroy the substrate surface.[24] Moreover, the corrosion products on the HDG surface had a tendency to form hydrozincite with immersion time, which was less protective than simonkolleite.[25] Therefore, the corrosion resistance of the HDG substrate did not maintain stability after 168 h of exposure to 0.1 M NaCl.

The electrochemical impedance diagrams of ZA and ZM samples showed two time constants in the investigated period. Similar to Nyquist plots for HDG substrate during immersion time, the ZA and ZM Nyquist plots presented

imperfect semicircles, which are related to physical phenomena such as roughness and surface inhomogeneity.[2] Besides, it can be seen that the heterogeneous corrosion product films from the SEM results (Figure 8); thus, the model $R_s(CPE_f(R_f(CPE_{dl}R_{ct})))$ was considered suitable for the EIS results (Figure 15a). Combining with the characterization results, the R_s was the solution resistance, R_f and CPE_f were related to the HT corrosion product layer, and R_{ct} and CPE_{dl} were associated with charge transfer resistance and the double layer capacitance. After 2 h, the R_f values of ZA and ZM substrates were 1366 and 1578 $\Omega\,cm^2$, respectively, which were not much different, compared to that of the HDG substrate (1167 $\Omega\,cm^2$). It indicated that the barrier properties of those corrosion product films were relatively

TABLE 5 Parameters of EIS for the HDG, ZA, and ZM substrates after exposure to 0.1 M NaCl.

Sample	CPE_f $(\Omega^{-1} s^n cm^{-2})$	n_f	R_f $(\Omega\ cm^2)$	CPE_{dl} $(\Omega^{-1} s^n cm^{-2})$	n	R_{ct} $(\Omega\ cm^2)$	$|Z|_{10\ mHz}$ $(\Omega\ cm^2)$
HDG—2 h	5.66×10^{-6}	0.89	1167	9.89×10^{-4}	0.94	1184	2378
HDG—24 h	-	-	-	2.31×10^{-4}	0.76	1409	1738
HDG—72 h	2.58×10^{-4}	0.82	2241	1.51×10^{-3}	0.9	877	2841
HDG—168 h	3.18×10^{-4}	0.78	1329	4.78×10^{-3}	0.81	401	1589
ZA—2 h	1.09×10^{-5}	0.78	1366	1.49×10^{-3}	0.84	1862	3419
ZA—24 h	3.23×10^{-4}	0.8	2072	7.59×10^{-3}	0.9	1430	2773
ZA—72 h	2.79×10^{-4}	0.84	3474	8.55×10^{-3}	0.9	1672	4457
ZA—168 h	3.12×10^{-4}	0.81	4466	4.14×10^{-3}	0.92	4680	6580
ZM—2 h	4.42×10^{-5}	0.78	1578	4.65×10^{-4}	0.62	4948	4351
ZM—24 h	1.75×10^{-4}	0.8	985	6.67×10^{-4}	0.6	1513	2691
ZM—72 h	2.67×10^{-4}	0.83	2773	3.79×10^{-3}	0.81	1683	3815
ZM—168 h	3.45×10^{-4}	0.84	5742	4.65×10^{-3}	0.88	6162	6185

Abbreviations: EIS, electrochemical impedance spectroscopy; HDG, hot-dip galvanized steel; ZA, Zn–Al-coated steel; ZM, Zn–Al–Mg-coated steel.
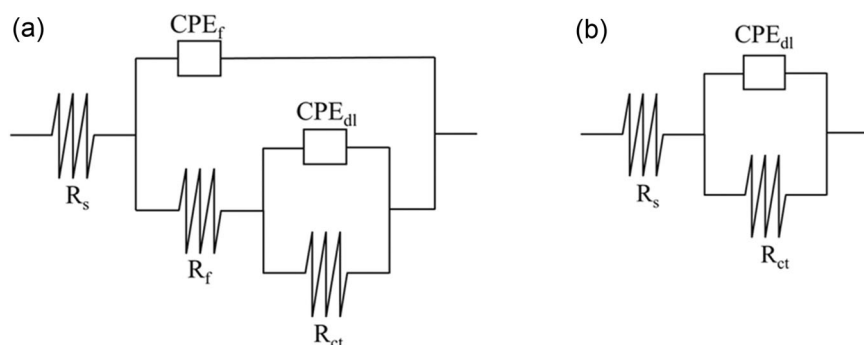
FIGURE 15 Equivalent circuit for the electrochemical impedance spectroscopy data fitting of the hot-dip galvanized steel, Zn–Al-coated steel, and Zn–Al–Mg-coated steel substrates.

similar. It was also seen that the ZM R_{ct} was the highest after 2h, the corrosion protection of the ZM substrate was sharply higher than those of the other two substrates, confirming that it provided more passive protection. The ZA and ZM R_f values rose obviously during immersion time (Table 5). The increase of R_f values was in complete agreement with the denser and better adhesion of the HT corrosion product films versus time (Figure 8) as a result, these HT films provided a higher covering ability for substrate surfaces. Moreover, the ZA and ZM R_f values were significantly higher than that of HDG one, which explained that the HT corrosion product films provided more protection than the simonkolleite film.[16,17] The R_{ct} values of the ZA and ZM substrates were reduced after 24 h, suggesting a decrease in the corrosion protection of those samples. This was due to the corrosion of the Zn-based surface substrates continuing at the anode areas.[2] However, the ZA and ZM R_{ct} values increased significantly after 72 and 168 h, which can attribute to the protective HT corrosion product films

(Table 5). The corrosion product films completely covered surfaces with immersion time and inhibited the zinc alloys dissolution with the prolonged immersion time, which also caused the decrease in ZA and ZM i_{corr} values.[2] Moreover, the previous research suggested that ZnAl-CO$_3$ HT acted as a physical protective layer, which isolated Cl$^-$ ions and the zinc-coated steel substrates.[20] The Cl$^-$ ions were also captured and restricted to move in these HT interlayers.[20] Combining the R_f values (Table 5) and SEM results (Figure 8), the significant improvement of the corrosion resistance of the ZA and ZM substrates can be elucidated based on the dense packing of corrosion product films.

3.4 | Discussion

From the characterization and surface morphology results, the corrosion mechanism and formation of corrosion products on all the zinc alloys were discussed
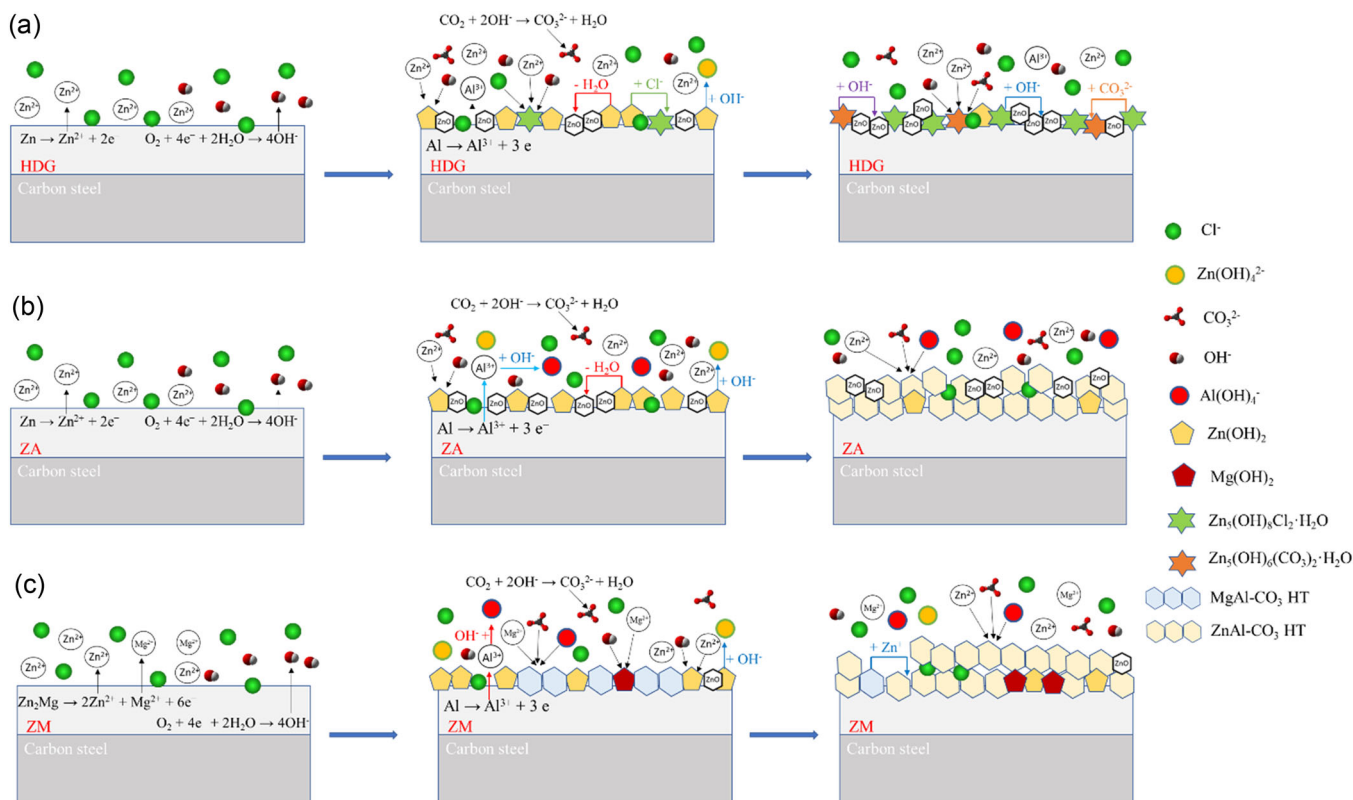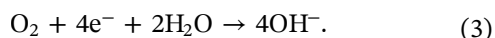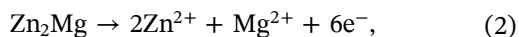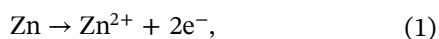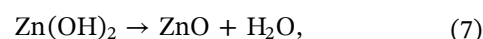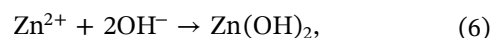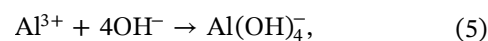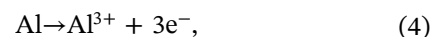
FIGURE 16 Corrosion process on the hot-dip galvanized steel (a), Zn–Al-coated steel (b), and Zn–Al–Mg-coated steel (c) substrates. [Color figure can be viewed at wileyonlinelibrary.com]
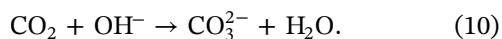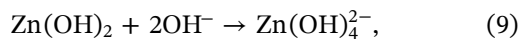
(Figure 16). The Zn phase of ZnAl alloys was preferentially dissolved during the corrosion process, while the Zn_2Mg phase of ZnAlMg alloys was the most active. Therefore, due to anodic reactions, only Zn^{2+} cations were formed (Equation 1) in the cases of HDG and ZA, in contrast, both Mg^{2+} and Zn^{2+} cations were provided (Equation 2) during the ZM corrosion.[7,10,15] The cathodic reaction corresponded to the reduction of oxygen in the Al-rich phase (Equation 3)[15]
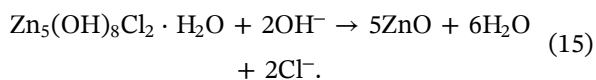
$$Zn \rightarrow Zn^{2+} + 2e^-, \tag{1}$$

$$Zn_2Mg \rightarrow 2Zn^{2+} + Mg^{2+} + 6e^-, \tag{2}$$
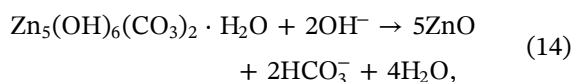
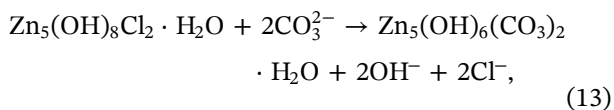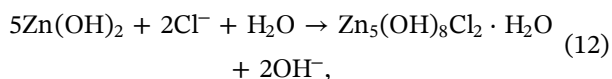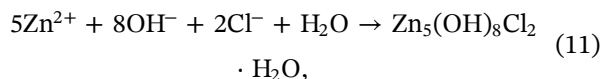$$O_2 + 4e^- + 2H_2O \rightarrow 4OH^-. \tag{3}$$

The reaction (Equation 3) led to the increase of local pH; thus, the Al phase began to dissolve (Equations 4 and 5) and the corrosion products were also formed on the substrate surface.[2,15] The Zn^{2+} cations reacted with OH^- anions resulting in the precipitation of $Zn(OH)_2$ (Equation 6) and eventually ZnO (Equation 7), whereas the Mg^{2+} cations formed $Mg(OH)_2/MgO$ (Equation 8).[7] As proved by previous

studies for the ZnMg and ZnAlMg alloy coatings, the presence of Mg^{2+} can contribute to the prevention of ZnO formation; thus, the dehydration of $Zn(OH)_2$ to form ZnO (Equation 7) was inhibited on the ZM surface.[18,23,26] Moreover, the Mg dissolution buffered the pH at cathodic regions; thus, they decreased the cathodic reaction and corrosion rate on the ZM surface.[18] It can be observed that the ZM R_{ct} after 2 h was sharply higher than those of two other substrates (Figure 14). Equation (3) reaction continuously happened, leading to a pH increase. Therefore, a part of $Zn(OH)_2$ can react with OH^- anions forming $Zn(OH)_4^{2-}$ (Equation 9).[2] The dissolution of carbon dioxide provided the amount of carbonate cations during the corrosion process (Equation 10)[26]

$$Al \rightarrow Al^{3+} + 3e^-, \tag{4}$$

$$Al^{3+} + 4OH^- \rightarrow Al(OH)_4^-, \tag{5}$$

$$Zn^{2+} + 2OH^- \rightarrow Zn(OH)_2, \tag{6}$$

$$Zn(OH)_2 \rightarrow ZnO + H_2O, \tag{7}$$

$$Mg^{2+} + 2OH^- \rightarrow Mg(OH)_2 \rightarrow MgO + H_2O, \tag{8}$$

$$Zn(OH)_2 + 2OH^- \rightarrow Zn(OH)_4^{2-}, \tag{9}$$

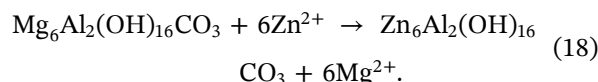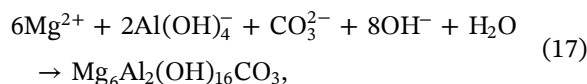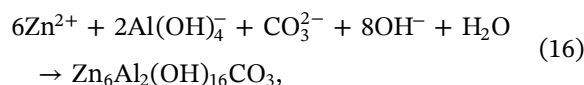$$CO_2 + OH^- \rightarrow CO_3^{2-} + H_2O. \tag{10}$$
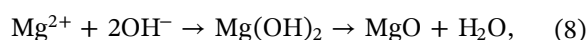
For the HDG sample, the simonkolleite formation was preferentially formed on the surface, following Equations (11) and (12) reactions, in the early steps of the corrosion process.[2,24] Then, the simonkolleite would react with HCO_3^- anions, transforming simonkolleite into zinc hydroxide carbonate in the later stage of the corrosion process (Equation 13).[26] Besides, the simonkolleite and zinc hydroxide carbonate can react with OH^- anions, generating ZnO when the pH solution rose (Equations 14 and 15).[15] Therefore, it was observed that the intensity of ZnO peaks increased obviously versus immersion time (Figure 5a). Because of the simonkolleite transformation into zinc hydroxide carbonate and ZnO, the corrosion products layer became more porous (Figure 8a) and the corrosion protection reduced significantly (Figure 14a,b) in the later step of the corrosion process

$$5Zn^{2+} + 8OH^- + 2Cl^- + H_2O \rightarrow Zn_5(OH)_8Cl_2 \\ \cdot H_2O, \tag{11}$$

$$5Zn(OH)_2 + 2Cl^- + H_2O \rightarrow Zn_5(OH)_8Cl_2 \cdot H_2O \\ + 2OH^-, \tag{12}$$

$$Zn_5(OH)_8Cl_2 \cdot H_2O + 2CO_3^{2-} \rightarrow Zn_5(OH)_6(CO_3)_2 \\ \cdot H_2O + 2OH^- + 2Cl^-, \tag{13}$$

$$Zn_5(OH)_6(CO_3)_2 \cdot H_2O + 2OH^- \rightarrow 5ZnO \\ + 2HCO_3^- + 4H_2O, \tag{14}$$

$$Zn_5(OH)_8Cl_2 \cdot H_2O + 2OH^- \rightarrow 5ZnO + 6H_2O \\ + 2Cl^-. \tag{15}$$

For the ZA and ZM samples, the HT formation was preferentially created on their surfaces, following the reactions in Equations (16) and (17).[7] Because the solubility constant of MgAl HT is lower than that of ZnAl HT, the MgAl HT was developed on the ZM surface in the early step of corrosion, which transformed into ZnAl HT by Mg^{2+} ions with Zn^{2+} ions in the next stages (Equation 18).[17] Besides, the dissolved Mg^{2+} ions can also stabilize the HT layer on the ZM surface during the corrosion process.[17] Therefore, it can be seen that a compact and dense HT layer has grown on the ZM surface during the surveyed period (Figure 8c) and the Mg concentration

on the ZM surface was reduced after exposure to 0.1 M NaCl for a longer time (Table 3). The Al concentration of the HDG surface substrate was low; thus, the amount of $Al(OH)_4^-$ was not enough to form ZnAl HT

$$6Zn^{2+} + 2Al(OH)_4^- + CO_3^{2-} + 8OH^- + H_2O \\ \rightarrow Zn_6Al_2(OH)_{16}CO_3, \tag{16}$$

$$6Mg^{2+} + 2Al(OH)_4^- + CO_3^{2-} + 8OH^- + H_2O \\ \rightarrow Mg_6Al_2(OH)_{16}CO_3, \tag{17}$$

$$Mg_6Al_2(OH)_{16}CO_3 + 6Zn^{2+} \rightarrow Zn_6Al_2(OH)_{16} \\ CO_3 + 6Mg^{2+}. \tag{18}$$

4 | CONCLUSION

The addition of Al and Mg elements in zinc alloy-coated steel substrates affected the deposition of their corrosion products on the surface and their corrosion resistance during immersion in NaCl solution. Based on the characterization and morphology results, a porous structure with poor adhesion to the surface such as simonkolleite and ZnO crystals was formed on HDG substrates; meanwhile, the ZnAl HT layer of corrosion product with density and adhesion was detected on the zinc alloy substrates with higher Al content such as ZA and ZM substrates during immersion in 0.1 M NaCl. Moreover, the presence of dissolved Mg^{2+} ions from the ZM surface provided a more compact and denser HT corrosion product layer and formed $Mg(OH)_2$/MgO corrosion products, interfering with the formation of ZnO. The electrochemical corrosion behavior results showed that the corrosion rate of these substrates was closely related to the formation of corrosion products. Because the presence of Al and/or Mg changed significantly both sacrificial protection to steel and the ZnAl HT formation, which provided a more protective layer than ZnO and simonkolleite, the ZA and ZM substrates offered decisively improved corrosion resistance in 0.1 M NaCl compared to HDG substrate. Besides, the corrosion resistance of the HDG substrate reduced sharply, while those of ZA and ZM increased strongly during exposure to 0.1 M NaCl.

DATA AVAILABILITY STATEMENT

Data that support the findings of this study are available from the corresponding author upon reasonable request.

ORCID

Thi Xuan Hang To http://orcid.org/0000-0002-4068-131X

Marie-Georges Olivier http://orcid.org/0000-0001-7771-7454

REFERENCES

[1] E. Berdimurodov, A. Kholikov, K. Akbarov, I. B. Obot, L. Guo, *J. Mol. Struct.* **2021**, *1234*, 130165.

[2] Y. Meng, L. Liu, D. Zhang, C. Dong, Y. Yan, A. A. Volinsky, L. N. Wang, *Bioactive Mater.* **2019**, *4*, 87.

[3] S. Schuerz, M. Fleischanderl, G. H. Luckeneder, K. Preis, T. Haunschmied, G. Mori, A. C. Kneissl, *Corros. Sci.* **2009**, *51*, 2355.

[4] J. Rodriguez, L. Chenoy, A. Roobroeck, S. Godet, M. G. Olivier, *Corros. Sci.* **2016**, *108*, 47.

[5] M. Mouanga, P. Berçot, J. Y. Rauch, *Corros. Sci.* **2010**, *52*, 3984.

[6] Y. Chen, W. Zhang, M. F. Maitz, M. Chen, H. Zhang, J. Mao, Y. Zhao, N. Huang, G. Wan, *Corros. Sci.* **2016**, *111*, 541.

[7] M. Salgueiro Azevedo, C. Allély, K. Ogle, P. Volovitch, *Corros. Sci.* **2015**, *90*, 472.

[8] E. Diler, B. Rouvellou, S. Rioual, B. Lescop, G. Nguyen Vien, D. Thierry, *Corros. Sci.* **2014**, *87*, 111.

[9] D. Thierry, N. LeBozec, A. Le Gac, D. Persson, *Mater. Corros.* **2019**, *70*, 2220.

[10] P. K. Rai, D. Rout, D. Satish Kumar, S. Sharma, G. Balachandran, *J. Mater. Eng. Perform.* **2021**, *30*, 4138.

[11] T. Weng, *Int. J. Electrochem. Sci.* **2018**, *13*, 11882.

[12] A. Al-Negheimish, R. R. Hussain, A. Alhozaimy, D. D. N. Singh, *Constr. Build. Mater.* **2021**, *274*, 121921.

[13] T. Prosek, J. Hagström, D. Persson, N. Fuertes, F. Lindberg, O. Chocholatý, C. Taxén, J. Šerák, D. Thierry, *Corros. Sci.* **2016**, *110*, 71.

[14] A. N. C. Costa, G. C. Silva, E. A. Ferreira, R. Z. Nakazato, *Res. Soc. Dev.* **2021**, *10*, e49810111973.

[15] Q. Huang, Y. Wang, B. Zhou, Y. Wei, F. Gao, T. Fujita, *Corros. Sci.* **2021**, *179*, 109165.

[16] J. Duchoslav, R. Steinberger, M. Arndt, T. Keppert, G. Luckeneder, K. H. Stellnberger, J. Hagler, G. Angeli, C. K. Riener, D. Stifter, *Corros. Sci.* **2015**, *91*, 311.

[17] P. Volovitch, T. N. Vu, C. Allély, A. Abdel Aal, K. Ogle, *Corros. Sci.* **2011**, *53*, 2437.

[18] D. Persson, D. Thierry, N. LeBozec, T. Prosek, *Corros. Sci.* **2013**, *72*, 54.

[19] T. Tsujimura, A. Komatsu, A. Andoh, in *Proc. 5th Int. Conf. Zinc and Zinc Alloy Coated Steel, GALVATECH'2001* (Ed. M. Lamberights), Centre de Recherches Metallurgiques (CRM), Brussels, Belgium **2001**, 145–152.

[20] T. T. Pham, T. D. Nguyen, A. S. Nguyen, Y. Paint, M. Gonon, T. X. H. To, M.-G. Olivier, *Surf. Coat. Technol.* **2022**, *429*, 127948.

[21] S. Peng, S.-K. Xie, F. Xiao, J.-T. Lu, *Corros. Sci.* **2020**, *163*, 108237.

[22] G. George, M. P. Saravanakumar, *Environ. Sci. Pollut. Res.* **2018**, *25*, 30236.

[23] S. Schürz, G. H. Luckeneder, M. Fleischanderl, P. Mack, H. Gsaller, A. C. Kneissl, G. Mori, *Corros. Sci.* **2010**, *52*, 3271.

[24] S. Li, B. Gao, S. Yin, G. Tu, G. Zhu, S. Sun, X. Zhu, *Appl. Surf. Sci.* **2015**, *357*, 2004.

[25] K. Bobzin, M. Oete, T. F. Linke, C. Schulz, *Mater. Corros.* **2015**, *66*, 520.

[26] P. Volovitch, C. Allely, K. Ogle, *Corros. Sci.* **2009**, *51*, 1251.